



HAL
open science

The use of fractional derivation in modeling ferroelectric dynamic hysteresis behavior over large frequency bandwidth

D. Guyomar, Benjamin Ducharne, G. Sebald

► **To cite this version:**

D. Guyomar, Benjamin Ducharne, G. Sebald. The use of fractional derivation in modeling ferroelectric dynamic hysteresis behavior over large frequency bandwidth. *Journal of Applied Physics*, 2010, 107 (11), pp.114108. 10.1063/1.3393814 . hal-02560961

HAL Id: hal-02560961

<https://hal.science/hal-02560961>

Submitted on 2 May 2020

HAL is a multi-disciplinary open access archive for the deposit and dissemination of scientific research documents, whether they are published or not. The documents may come from teaching and research institutions in France or abroad, or from public or private research centers.

L'archive ouverte pluridisciplinaire **HAL**, est destinée au dépôt et à la diffusion de documents scientifiques de niveau recherche, publiés ou non, émanant des établissements d'enseignement et de recherche français ou étrangers, des laboratoires publics ou privés.

The use of fractional derivation in modeling ferroelectric dynamic hysteresis behavior over large frequency bandwidth

D. Guyomar, B. Ducharme, and G. Sebald

Citation: *J. Appl. Phys.* **107**, 114108 (2010); doi: 10.1063/1.3393814

View online: <http://dx.doi.org/10.1063/1.3393814>

View Table of Contents: <http://jap.aip.org/resource/1/JAPIAU/v107/i11>

Published by the [American Institute of Physics](#).

Related Articles

Evolution of polar order in $(1-x)\text{Pb}(\text{In}_{1/2}\text{Nb}_{1/2})\text{O}_3-x\text{PbTiO}_3$ ($0 \leq x \leq 1$) system as investigated by dielectric and Raman spectroscopy

J. Appl. Phys. **113**, 074101 (2013)

An in situ diffraction study of domain wall motion contributions to the frequency dispersion of the piezoelectric coefficient in lead zirconate titanate

Appl. Phys. Lett. **102**, 042911 (2013)

Two dimensional ferroelectric domain patterns in Yb^{3+} optically active LiNbO_3 fabricated by direct electron beam writing

Appl. Phys. Lett. **102**, 042910 (2013)

Local probing of the interaction between intrinsic defects and ferroelectric domain walls in lithium niobate

Appl. Phys. Lett. **102**, 042905 (2013)

Structural investigation of interface and defects in epitaxial $\text{Bi}_{3.25}\text{La}_{0.75}\text{Ti}_3\text{O}_{12}$ film on $\text{SrRuO}_3/\text{SrTiO}_3$ (111) and (100)

J. Appl. Phys. **113**, 044102 (2013)

Additional information on *J. Appl. Phys.*

Journal Homepage: <http://jap.aip.org/>

Journal Information: http://jap.aip.org/about/about_the_journal

Top downloads: http://jap.aip.org/features/most_downloaded

Information for Authors: <http://jap.aip.org/authors>

ADVERTISEMENT



AIP Advances

Now Indexed in Thomson Reuters Databases

Explore AIP's open access journal:

- Rapid publication
- Article-level metrics
- Post-publication rating and commenting

The use of fractional derivation in modeling ferroelectric dynamic hysteresis behavior over large frequency bandwidth

D. Guyomar, B. Ducharne,^{a)} and G. Sebald

*Laboratoire de Génie Electrique et Ferroélectricité—INSA de Lyon, Bât. Gustave FERRIE,
8 rue de la Physique, 69621 Villeurbanne Cedex, France*

(Received 10 June 2009; accepted 21 March 2010; published online 7 June 2010)

The present article proposes a dynamical model to obtain ferroelectric hysteresis dynamics based on fractional derivatives. The consideration of a fractional derivative term widely increases the frequency bandwidth of the accuracy of the traditional hysteresis models. As a consequence, the model is suited for successfully taking into account the well-known scaling relations of the ferroelectric hysteresis area, $\langle A \rangle$, versus the frequency, f , and field amplitude, E_0 . Under low frequency excitation, simulation tests provided good results regarding the comparison of the fractional model, experimental results and the well-known nonentire power law $\langle A \rangle \propto f^{1/3} E_0^{2/3}$ (where $\langle A \rangle$ represents the hysteresis loop area). These results were followed by comparing the hysteresis area obtained from the fractional model with that from the well known scaling relations as $f \rightarrow \infty$, and the results were proposed as validation of the high frequency behavior. Next, the model was tested on large frequency bandwidths (>6 decades) and validated with success using the comparison between simulation tests and the only experimental results available in literature obtained in such conditions by Liu *et al.* [J. Phys.: Condens. Matter **16**, 1189 (2004)] for BNT thin film samples.

© 2010 American Institute of Physics. [doi:10.1063/1.3393814]

I. INTRODUCTION

During the past twenty years, the hysteresis area, $\langle A \rangle$, has been widely studied as a function of the frequency of a time-varying external field, and represents a major support for the characterization of numerous industrial applications.^{1,2} $\langle A \rangle$ is related to both the energy dissipation in one cycle of domain reversal and the nonequilibrium first-order phase transitions in ferroelectrics. It represents the energy dissipation (loss) in one cycle of spin order reversal through irreversible domain wall migration (nucleation and growth). In a general way, the hysteresis is formed due to the relaxation delay of the system responding to the external field.^{3,4}

Modeling dynamic hysteresis properties over wide range of excitation frequencies have been widely studied and presented in the literature. By instance, for ferromagnetic materials, two-dimensional Ising models^{5,6} have been used to describe magnetic hysteresis versus varying frequency but they are usually not fully consistent with the experimental results. Other models as extended Preisach models with differential equations correctly behave but unfortunately through a frequency bandwidth usually restricted to three decades of frequency.⁷ Lead zirconate titanate $\text{PbZr}_{1-x}\text{Ti}_x\text{O}_3$ (PZT) ceramics have been extensively employed in a large number of industrial applications, particularly in the case of donor-doped PZT with a soft piezoelectric behavior. The understanding and modeling of dynamic hysteresis behaviors permits the computation of dissipation losses and dielectric responses of ferroelectric devices (such as piezoelectric actuators).⁸ Recently, several research efforts have been re-

ported on $\text{SrBi}_2\text{Ta}_2\text{O}_9$ (SBT) and $\text{Bi}_{3.15}\text{Nd}_{0.85}\text{Ti}_3\text{O}_{12}$ (BNT) thin films with varying Nd compositions. Such materials present much interest as they are particularly well suited for nonvolatile random access memory (NvRAM) applications.^{9,10}

By understanding and modeling the $\langle A \rangle$ versus the frequency, f , and electrical field amplitude, E_0 , one may predict the performances of ferroelectric thin films as used in NvRAM devices. Physically, it also becomes possible to understand the dynamics of domain reversal, in particular the characteristic times of domain nucleation and domain boundary motion as concurrent processes during the domain reversal. Finally, the dynamical hysteresis behavior is universal to every physical spinlike system, e.g., ferromagnetic materials exhibit similar dynamic activities.^{11–13} The exposed theory, at first developed for dielectric materials, can be universally applied to other classes of spinlike systems.

Numerous theoretical studies have described the scaling law of the hysteresis area as a function of f and E_0 , i.e., $\langle A \rangle \propto f^{\mu_1} E_0^{\mu_2}$ (where μ_1 and μ_2 are real parameters depending on the geometry and the nature of the system). It is necessary to understand and interpret these scaling behaviors in order to predict the characteristics of ultrahigh-frequency ceramics. As a result of the high power required at these frequency levels, the measured information is usually limited. The three-dimensional models [$(\emptyset^2)^2$ and $(\emptyset^2)^3$], from Rao *et al.*, were based on the study of the magnetic hysteresis in model continuum and lattice spin systems, and have given rise to two scaling relations applicable to low- f and high- f limits,^{10,13} i.e.,:

$$\langle A \rangle \propto f^{1/3} E_0^{2/3} \quad \text{as } f \rightarrow 0 \quad (1)$$

^{a)}Author to whom correspondence should be addressed. Electronic mail: benjamin.ducharne@insa-lyon.fr.

$$\langle A \rangle \propto f^{-1} E_0^2 \quad \text{as } f \rightarrow \infty \quad (2)$$

Other scaling relations for ferroelectric materials have been proposed by Yimnirun *et al.*,^{4,8,14–16} and Liu *et al.*¹⁷ have reported on relations for ferroelectric thin films. In these cases, the μ_1 and μ_2 values were adapted to the new supports. On a large frequency bandwidth, the curve $\langle A \rangle(\text{freq})$ exhibited a single-peak pattern for which both the value of the peak and the peak position increased as E_0 was raised. Scaling relations have been also used to describe the scaling behavior in the so-called “subcoercive” conditions, pointed out in more recent literature.^{15,16} A future paper will describe how our fractional model gives good agreement under such particular conditions. Scaling laws were developed as a first attempt to tackle investigations on those behaviors, and frequency exponent of 0.3 up to 0.6 were found. It is an interesting way to understand losses in ferroelectrics but this doesn't constitute a model suitable for modeling ferroelectric behavior. Other approaches have been developed mainly to be used as a dynamical inverse hysteresis model for the control of piezoelectric actuators. These inverse models are often based on a Preisach model of hysteresis^{18–20} or on a “generalized Maxwell slip” (GMS) model of hysteresis.²¹ Other approaches have been investigated, using a neural network²² or a phase shifting operator²³ for hysteresis compensation. But due to the specificity of piezoelectric actuators, all of these approaches exhibit usually various limitations (amplitude, frequency, etc.) and can only be used in the field of the associated application.

Within the framework of previous research efforts, we have previously proposed a novel formulation based on non-entire derivatives for modeling dynamic hysteresis on a large frequency bandwidth (i.e., over four frequency decades).^{24–26} The study was devoted to the modeling of the frequency dependence of the loop area, $\langle A \rangle$, the coercive field, E_c , (as a shape parameter) and the dielectric permittivity, ϵ_{33} , and good results were obtained.

The proposed theoretical model comprises two important terms: a static contribution, with the form of a damping force (a negative first-order polarization time derivative corresponding to the poling current); and a time-dependent loss term, constituted of the product of a material constant, ρ , and a fractional polarization derivative term, $d^\alpha P / dt^\alpha$ ($\alpha \in \mathbb{R}$). The work presented herein explains how, by using the model, it is possible to successfully reproduce the asymptotic evolutions of the previously-mentioned well-known scaling functions over a full frequency span.

II. MODEL

A. Quasistatic contribution

A static contribution signifies observing a looplike hysteresis when plotting the spontaneous polarization, P versus E for very low frequencies ($f \ll 1$ Hz). At such frequency levels, wall movements are assumed to undergo a mechanical-like dry friction.^{27,28} A static (frequency-independent) equation based on its mechanical dry-friction counterpart has been established in order to account for this property. The generation of a major $P(E)$ hysteresis loop was

obtained with good approximation by translating an anhysteretic curve. The loop also depended on the sign of the time derivative of the polarization. This translation was equal to the coercive field, E_c .

$$\begin{aligned} \text{if: } E(t) > f^{-1}[P(t)] + E_c, \\ P(t + dt) &= f[E(t + dt) - E_c], \\ \text{if: } E(t) < f^{-1}[P(t)] - E_c, \\ P(t + dt) &= f[E(t + dt) + E_c], \\ \text{if: } f^{-1}[P(t)] - E_c < E(t) < f^{-1}[P(t)] + E_c, \\ P(t + dt) &= P(t). \end{aligned} \quad (3)$$

Until electric field E reaches the coercive field E_c , the polarization remains constant. An electrical displacement occurs as soon as E exceeds E_c . After the field reaches E_{max} and reversing the field the polarization remains constant until E gets below $E_{\text{max}} - 2E_c$, and so on. This explanation is very close to the static friction used in mechanics.

Here, $f(E)$ (reciprocally $f^{-1}(P)$) represents the behavior of a nonlinear dielectric (without hysteresis), and the function can be obtained by fitting the parameters γ, σ to the anhysteretic curve of a perfect dielectric function, e.g.,

$$f(E) = \sigma \tan^{-1}\left(\frac{E}{\gamma}\right) \quad f^{-1}(P) = \gamma \tan\left(\frac{P}{\sigma}\right) \quad (4)$$

Equation (3) gives a correct description of the major hysteresis loops observed during steady state of the ceramic under a high-amplitude electrical field ($E_0 \gg E_c$). On the other hand, the polarization remained null until the value of the electric field became equal to that of the coercive field. This signifies that the first polarization curve could not be correctly reproduced by the first equation, which was true for all simulated minor loops. It was thus concluded that Eq. (3) was ineffective for loops observed under asymmetrical excitation field waveforms (e.g., first polarization curve, minor loops, etc.).

A good global ferroelectric material model needs to take into account the set of similar behaviors of each domain wall and is characterized by its coercive field. More realistic cycles, including minor loops, are obtained by introducing a distribution of a basic element (spectrum), characterized by its own coercive fields in addition to its own weight. The most general set of equations for the model, including losses, is given below. Here, for a quasistatic case, $\rho_1 = 0$.

$$\begin{aligned} \text{if: } E(t) > f^{-1}[P_i(t)] + E_{c_i} + \rho_1 \cdot \frac{d^\alpha P_i(t)}{dt^\alpha}, \\ P_i(t + dt) &= f\left(E(t + dt) - E_{c_i} - \rho_1 \cdot \frac{d^\alpha P_i(t)}{dt^\alpha}\right), \\ \text{if: } E(t) < f^{-1}[P_i(t)] - E_{c_i} + \rho_1 \cdot \frac{d^\alpha P_i(t)}{dt^\alpha}, \end{aligned}$$

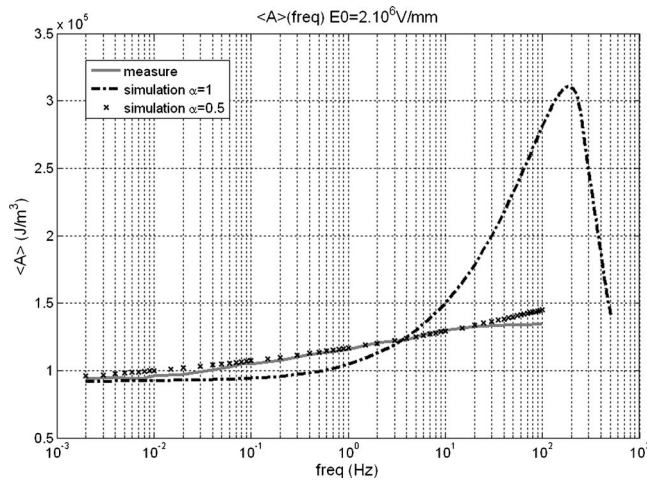


FIG. 1. A comparison between a simulated and measured $\langle A \rangle(f)$ curve.

$$P_i(t+dt) = f\left(E(t+dt) + Ec_i - \rho_1 \cdot \frac{d^\alpha P_i(t)}{dt^\alpha}\right),$$

$$\text{if: } f^{-1}[P_i(t)] - Ec_i + \rho_1 \cdot \frac{d^\alpha P_i(t)}{dt^\alpha} < E(t) < f^{-1}[P_i(t)] + Ec_i$$

$$+ \rho_1 \cdot \frac{d^\alpha P_i(t)}{dt^\alpha} + P_i(t+dt)$$

$$= P_i(t) \sum_{i=1}^k \text{Spectrum}(i) \cdot P_i = P. \quad (5)$$

The function $\text{Spectrum}(i)$ represents the distribution of elementary loops. The protocol that was established in order to obtain this distribution²⁵ involving, first, determining an experimental anhysteretic curve. The parameters γ and k were obtained when $f^{-1}(P)$ matched the anhysteretic curve (by way of an identification algorithm using the Matlab[®] curve fitting toolbox). The spectrum distribution was obtained through deconvolution of the measured first polarization curve by the previously obtained anhysteretic curve. Based on this process, it was possible to systematically establish the static parameters of the material. A large number of results as well as further information concerning the static model is available elsewhere.^{24,26}

B. Dynamic considerations

Beyond the quasistatic limit, ferroelectric materials exhibit hysteresis loops that are strongly dependent on the frequency. These states of dependence were clearly considered in the scaling laws of Eqs. (1) and (2). As reported in previous papers,^{24,26} the dynamical effect is usually considered as an equivalent dissipative field derived from an Ohm's resistivity, ρ , and in system 5, this corresponds to $\alpha=1$.

As explained in²⁴ and illustrated in Fig. 1, this dynamical modeling was accurate for a restrained frequency bandwidth. The identification of the parameter ρ that perfectly fit the low frequency part of the $\langle A \rangle(\text{freq})$ curve led to an over-contribution of the dynamical term $\rho \cdot dP/dt$ for the high frequency part of the curve. Reciprocally, by adjusting the pa-

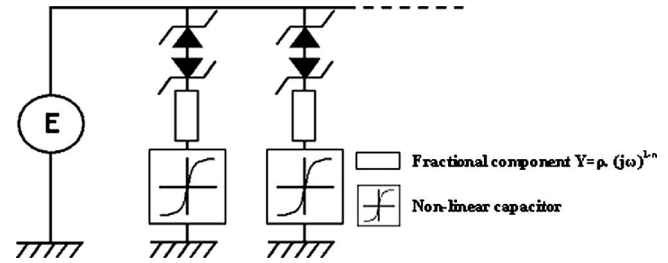


FIG. 2. Electrical analog circuit of the dynamical model.

rameter ρ on the high frequency component of the curve, one can observe large differences between simulated and measured results as $f \rightarrow 0$.

This overestimation was corrected in²⁶ by defining a nonentire operator balancing the low and high frequency components differently as opposed to a linear time derivative.

An nonentire derivation generalizes the concept of derivative to noninteger orders. The order of the derivation is not restricted to an entire but can be a real or a complex number.^{29,30} The fractional derivation of a function $f(t)$ is the convolution between the $f(t)$ function and $t^\alpha H(t)/\Gamma(1-\alpha)$ where $\Gamma(\alpha)$ is the gamma function and α the order of fractional derivation. From a spectral point of view, the fractional derivation means that the frequency spectrum $f(\omega)$ of $f(t)$ will be multiplied by $(j\omega)^\alpha$ in place of $j\omega$ for a first order derivation. It physically means that the computation of the present instant $f(t)$ not only required the previous instant $f(t-dt)$ but all the past history.

In the present study, dynamical unsymmetrical hysteresis loops were obtained by introducing the fractional operator into system 5, i.e., $\alpha \neq 0$.

The new dynamical contribution $\rho \cdot d^\alpha P/dt^\alpha$ gave rise to a significant increase in the accuracy as illustrated in the loop area versus frequency curve (Fig. 1) obtained for the given E_0 .

Figure 2 is an illustration of the analog electrical circuit of the model. The fractional component exhibits an admittance written as $Y = \rho \cdot (j\omega)^{1-\alpha}$ ($0 < \alpha < 1$). Its behavior is opposite to the behavior of usual constant phase elements, when n is close to zero the fractional component reacts as an equivalent capacitor and when n is close to one it reacts as an equivalent resistor.

III. SCALING LAWS CONSIDERATIONS

As portrayed in Fig. 1, on bulk ceramics the measuring range for the frequency is usually limited to 100 Hz under a high electrical field ($E_0 > 2 \times 10^6$ V/m). This limitation is due to the power amplifier that is unable to deliver the required current. Liu *et al.*¹⁰ have demonstrated on thin films that, for a large frequency bandwidth (>6 decades), the loop area first increases up to a maximum value that depends on the electrical field amplitude. As E_0 experiences arise, $\langle A \rangle \times (f)$ also increases, with the peak position and height shifting to the right and upward, respectively. Subsequently, the loop area quickly decreases to a value close to zero for very high frequencies. As shown in Fig. 3(A), the hysteresis loop

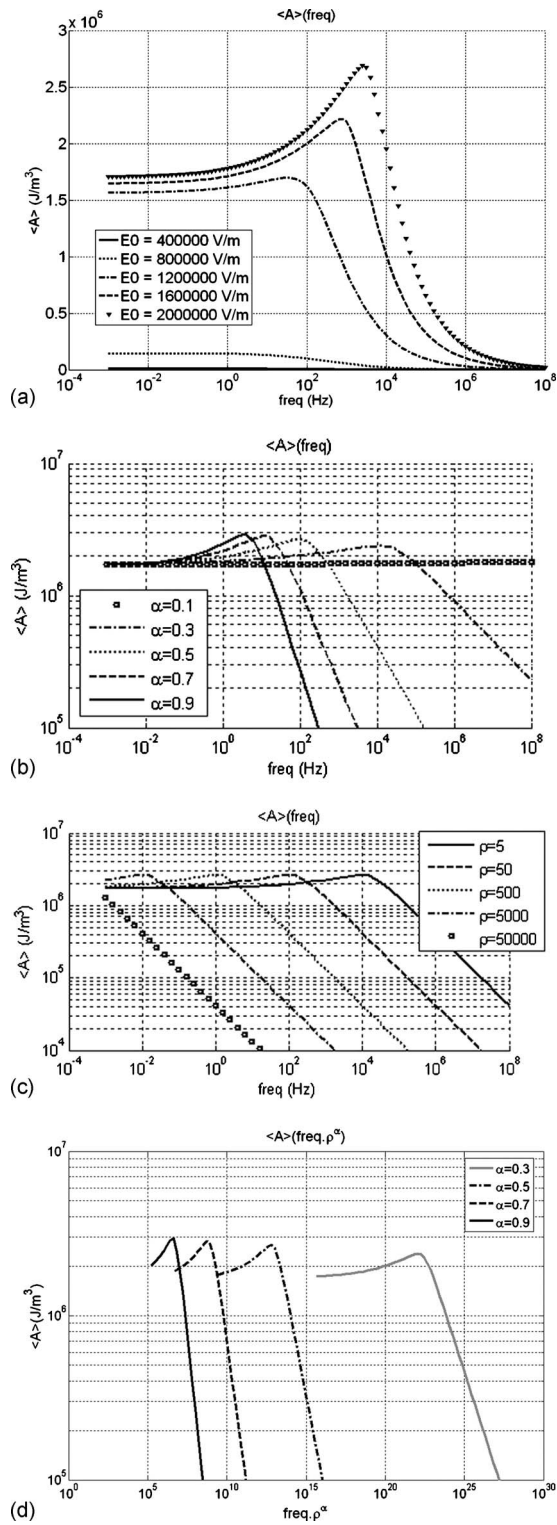


FIG. 3. (A) The hysteresis area $\langle A \rangle$ vs the frequency for various values of the maximum electrical field E_0 ($\alpha=0.5$, $\rho=10$). (B) The hysteresis area $\langle A \rangle$ vs the frequency for various values of the fractional order α . (C) The hysteresis area $\langle A \rangle$ vs the frequency for various values of the parameter ρ . (D) The hysteresis area $\langle A \rangle$ vs the product of the frequency and the parameter $\rho^{1/\alpha}$.

area shows a peak after decreasing to zero. Moreover, the peak amplitude depends on electric field as shown experimentally by Liu *et al.*¹⁰ The following figures show then how to modify the curves shape by changing the different parameters of the fractional derivative term.

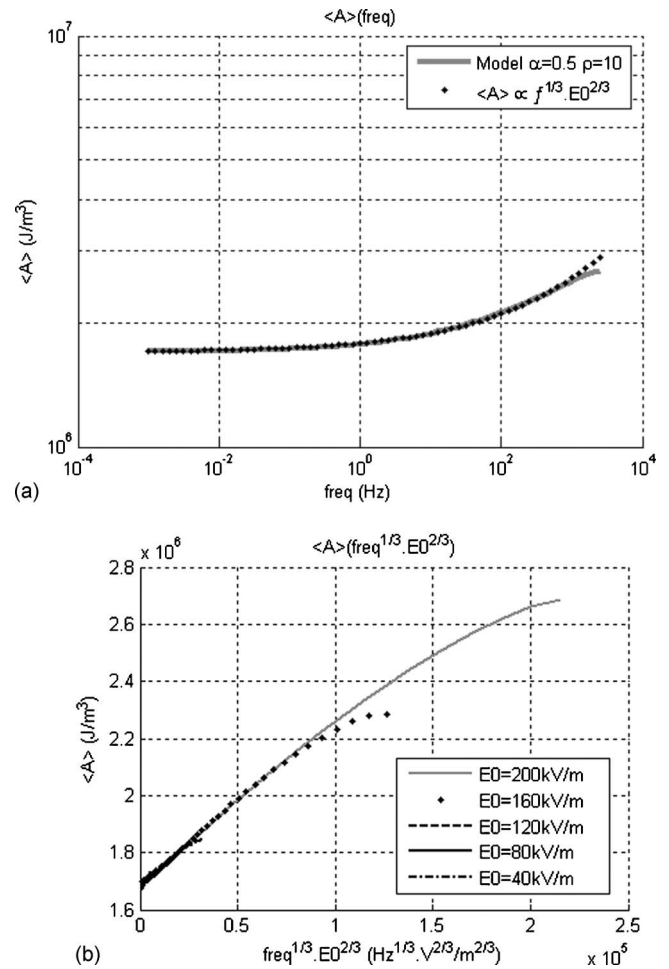


FIG. 4. A comparison between the fractional model and scaling law as $f \rightarrow 0$.

In Fig. 3(B), one can see that, for a decreasing α , the peak of $\langle A \rangle$ appears at a higher frequency and the rates of the increasing and decreasing part of the curve are weaker.

Figure 3(C) illustrates the influence of ρ on the position of the maximum value of $\langle A \rangle$. In this case, the rates of the increasing and decreasing parts of the curve remain constant, and a scaling relation can be proposed. A single curve was obtained for a given α while plotting $\langle A \rangle$ versus the product of the frequency and the parameter $\rho^{1/\alpha}$ [Fig. 3(D)].

Finally, it can be stated that the position of the peak of the $\langle A \rangle$ (freq) curve was dependent on both ρ and α , whereas the rate of the increasing and decreasing parts was only dependant on α . Simulation results on a typical industrial, soft PZT composition (P188 obtained from quartz and silica, France type Navy II) allowed the setting and validation of this coefficient to 0.5 as $f \rightarrow 0$.^{24,26} Furthermore, Fig. 4 illustrates that the scaling relation proposed by Rao¹³ was particularly well suited for the frequency range 10^{-3} –100 Hz.

Rao *et al.*¹³ were the first to scale the decreasing part by using Eq. (2) ($\langle A \rangle \propto f^{-1} E_0^2$ as $f \rightarrow \infty$) on magnetic materials, other scaling relations are available:

- $\langle A \rangle \propto f^{-2/3} E_0^2$ proposed by Liu *et al.*³¹ for ferroelectric thin films.
- $\langle A \rangle \propto f^{-1/4} E_0$ proposed by Yimnirun *et al.*⁸ for soft PZT bulk ceramics.

These scaling relations indicate that, depending on the tested material, the influence of f and E_0 on the variation in the hysteresis area, $\langle A \rangle$, will not have the same weight. Yimnirun *et al.* linked these differences to the various energy levels required for the polarization flip. The exponent for the E_0 -term was linked to the polarization-flip kinetics, whereas the f exponent was dependent on the depolarizing level through the tested sample.⁴ A high depolarizing factor resulted in a relatively weak dependence on f of the hysteresis area, $\langle A \rangle$. The three scaling relations proposed for varying types of materials gave rise to the different simulation results as it is the case in Fig. 3(b).

When $f \rightarrow \infty$, the rate of the logarithmic $\langle A \rangle$ versus freq. curve became directly linked to the nonentire derivative coefficient, α . In the scaling relations, $f^{\mu_1} E_0^{\mu_2}$, $\mu_1 = -\alpha$ provided the rate of the curve and μ_2 gave the amplitude (i.e., the value at the origin). After spectrum analysis, it can be noted that the peak position was given by: $\omega_0 = (1/U)^{1/\alpha}$ where U is a constant equal to Resistor, Capacitor (RC) in a first-order differential system.

To conclude, the rates of the increasing and decreasing parts of the $\langle A \rangle$ versus freq. curve were highly dependent on the fractional coefficient, and by setting this coefficient to 0.5 as $f \rightarrow 0$ (i.e., for mechanical creep, measurement of hysteresis loops), it was possible to determine the peak position and the rate of the decreasing part.

As a final validation of the model, a comparison has been done between the experimental results obtained by Liu *et al.*¹⁰ and the fractional model. These experimental results were obtained for a large frequency bandwidth (1 to 10^6 Hz) for Nd-substituted $\text{Bi}_4\text{Ti}_3\text{O}_{12}$ thin films. The electrical field E_0 range is 100–400 kV/cm. The characterization of the samples has been done using Sawyer–Tower circuit. As the shapes of the hysteresis loops and the physical behaviors are different to the ceramic sample P188 previously used to define the model, a new set of parameters is necessary. In the case of $\text{Bi}_{3.15}\text{Nd}_{0.85}\text{Ti}_3\text{O}_{12}$, Liu and al thin film samples, the best results were obtained with $\alpha = 0.4$, $\rho = 7 \times 10^5$.

As it has already been observed as $f \rightarrow 0$ and $\rightarrow \infty$, we notice good fitting between the fractional model and the measures for large frequency bandwidth type excitation. It is particularly interesting to conclude that a single set of parameters allows to perfectly reproduce the characteristics tendencies of the $\langle A \rangle(\text{freq})$ curves (increasing rates, peak position, decreasing last part, etc.), we prove here that an only fractional operator is sufficient to take into account with success all the dynamical behaviors of a ferroelectric material ($f \in [10^{-3}; 10^6]$ Hz) (Fig. 5).

IV. DISCUSSION AND CONCLUSIONS

In summary, the dynamic hysteresis stability for ferroelectric PZT materials was investigated. From the obtained results, it was possible to develop a theoretical model based on two independent contributions such as:

(1) A quasi static contribution, mathematically similar to dry friction equations and physically linked to wall movement.

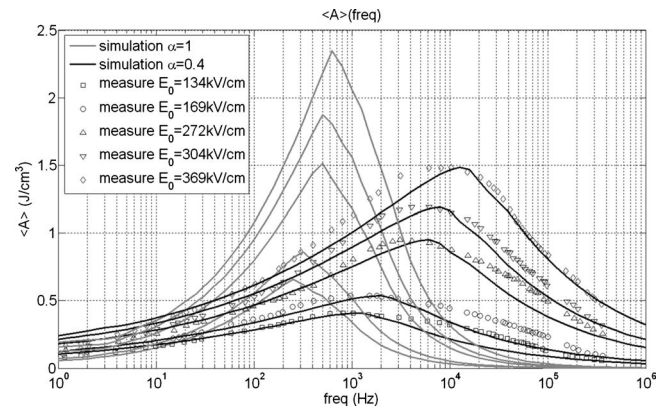


FIG. 5. Comparison between Liu experimental results and model on $\langle A \rangle \times (\text{freq})$ curves for different values of E_0 and α .

(2) A dynamical contribution, given by fractional derivative term that represents “viscous” losses.

Power-law frequency dependences, i.e., $\langle A \rangle \propto E_0^{2/3} f^\mu$ ($\mu \in [0; 1]$) over the low-frequency range and $\langle A \rangle \propto E_0^2 f^\mu$ ($\mu \in [-2; 0]$) over the high-frequency range, are usually proposed for the characterization of a dynamic hysteresis. The value of α , which represents the order of the fractional term, was set equal to 0.5, which rendered it possible to successfully reproduce the material behavior as $f \rightarrow 0$, (as illustrated with experimental results in Fig. 1) and with a scaling relation in Fig. 4. By maintaining α equal to 0.5, a high-frequency behavior (peak position and decreasing rate of the $\langle A \rangle(\text{freq})$ curve) was then determinate by simulation.

To conclude, the introduction of a nonentire derivative term to the model permitted a significant increase in the frequency bandwidth (>6 decades), to our knowledge, this is the only way to get an accurate modeling on such frequency span.

Future research will be dedicated to extending the model in order to incorporate additional excitations, such as mechanical stress. The influence of such combined effects on dynamical wall movements, as well as on the behavior of other fundamental coefficients, such as the piezoelectric coefficient, d_{33} , the dielectric permittivity, ϵ_{33} , and the elastic compliance, s_{33} , will also be investigated.

¹K. Uchino, *Ferroelectric Device* (Marcel Dekker Inc., New York, 2000), p. 145.

²B. Jaffe, W. R. Cook, and H. Jaffe, *Piezoelectric Ceramics* (Academic, London, 1971).

³B. Pan, H. Yu, D. Wu, X. H. Zhou, and J.-M. Liu, *Appl. Phys. Lett.* **83**, 1406 (2003).

⁴R. Yimnirun, Y. Laosiritaworn, S. Wongsanmai, and S. Ananta, *Appl. Phys. Lett.* **89**, 162901 (2006).

⁵S. W. Sides, P. A. Rikvold, and M. A. Novotny, *J. Appl. Phys.* **83**, 6494 (1998).

⁶M. Acharyya and B. K. Chakrabarti, *Phys. Rev. B* **52**, 6550 (1995).

⁷X. Tan and J. S. Baras, *Automatica* **40**, 1469 (2004).

⁸R. Yimnirun, R. Wongmaneeerung, S. Wongsanmai, A. Ngamjarrojana, S. Ananta, and Y. Laosiritaworn, *Appl. Phys. Lett.* **90**, 112908 (2007).

⁹C. A. Paz de Araujo, J. D. Cuchiaro, L. D. McMillan, M. C. Scott, and J. F. Scott, *Nature* **374**, 627 (1995).

¹⁰J. M. Liu, B. Pan, H. Yu, and S. T. Zhang, *J. Phys.: Condens. Matter* **16**, 1189 (2004).

¹¹D. C. Jiles and D. L. Atherton, *J. Magn. Magn. Mater.* **61**, 48 (1986).

¹²G. Bertotti, *Hysteresis in Magnetism* (Academic Press, Torino, 1998).

- ¹³M. Rao, H. R. Krishnamurthy, and R. Pandit, *Phys. Rev. B* **42**, 856 (1990).
- ¹⁴R. Yimnirun, Y. Laosiritaworn, S. Ananta, and S. Wongsanmai, *Appl. Phys. Lett.* **89**, 242901 (2006).
- ¹⁵R. Yimnirun, R. Wongdamnern, N. Triamnak, T. Sareein, M. Unruan, A. Ngamjarrojana, S. Ananta, and Y. Laosiritaworn, *J. Phys. D* **41**, 205415 (2008).
- ¹⁶R. Yimnirun, R. Wongdamnern, N. Triamnak, M. Unruan, A. Ngamjarrojana, S. Ananta, and Y. Laosiritaworn, *J. Phys.: Condens. Matter* **20**, 415202 (2008).
- ¹⁷J.-M. Liu, H. L. W. Chan, C. L. Choy, Y. Y. Zhu, S. N. Zhu, Z. G. Liu, and N. B. Ming, *Appl. Phys. Lett.* **79**, 236 (2001).
- ¹⁸P. Ge and M. Jouaneh, *IEEE Trans. Control Syst. Technol.* **4**, 209 (1996).
- ¹⁹A. Cavallo, C. Natale, S. Pirozzi, and C. Visone, *IEEE Trans. Magn.* **39**, 1389 (2003).
- ²⁰G. Song, J. Q. Zhao, X. Q. Zhou, and J. A. De Abreu-Garcia, *IEEE/ASME Trans. Mechatron.* **10**, 198 (2005).
- ²¹P. Mayhan, K. Srinivasan, S. Watechagit, and G. Washington, *J. Intell. Mater. Syst. Struct.* **11**, 771 (2000).
- ²²S. Yu, B. Chirinzadeh, G. Alici, and J. Smith, Proceedings of IEEE International Conference on Robotics and Automation, Vols. 1–4, p. 3641 (2005).
- ²³J. M. Cruz-Hernandez and V. Hayward, *IEEE Trans. Control Syst. Technol.* **9**, 17 (2001).
- ²⁴D. Guyomar, B. Ducharne, and G. Sebald, *J. Phys. D* **41**, 125410 (2008).
- ²⁵D. Guyomar, B. Ducharne, and G. Sebald, *J. Phys. D* **40**, 6048 (2007).
- ²⁶D. Guyomar, B. Ducharne, and G. Sebald, *IEEE Trans. Ultrason. Ferroelectr. Freq. Control* **56**, 437 (2009).
- ²⁷B. Ducharne, D. Guyomar, and G. Sebald, *J. Phys. D* **40**, 551 (2007).
- ²⁸G. Sebald, E. Boucher, and D. Guyomar, *J. Appl. Phys.* **96**, 2785 (2004).
- ²⁹A. K. Grünwald, *Z. Angew. Math. Phys.* **12**, 441 (1867).
- ³⁰B. Riemann, *Gesammelte Werke* (Dover, Leipzig, 1892).
- ³¹J. M. Liu, Q. Xiao, Z. G. Liu, H. L. W. Chan, and N. B. Ming, *Mater. Chem. Phys.* **82**, 733 (2003).